WILEY-VCH

Synthesis and biological evaluation of a new class of mitochondria-targeted gadolinium(III) agents

Daniel E. Morrison,[a] Jade B. Aitken,[a] Martin D. de Jonge,[b] Fatiah Issa,[a] Hugh H. Harris[c] and Louis M. Rendina*[a]

Abstract: A structure-activity relationship (SAR) study of a library of novel bifunctional Gd(III) complexes covalently linked to arylphosphonium cations is reported. Such complexes have been designed for potential application in cutting-edge binary cancer therapies such as neutron capture therapy (NCT) and photon activation therapy (PAT). A positive correlation was found between lipophilicity (log$P$) and cytotoxicity (IC$_{50}$) of the complexes. Mitochondria uptake was determined by means of ICP-MS, and Gd uptake was determined by means of quantification using synchrotron X-ray fluorescence (XRF) imaging. A negative correlation between lipophilicity and tumor selectivity of the Gd(III) complexes was demonstrated. This study highlights the delicate balance required in order to minimise *in vitro* cytotoxicity and optimise *in vitro* tumor selectivity and mitochondrial localisation for this new class of mitochondria-targeted binary therapy agents. We also report the highest *in vitro* tumor selectivity for any Gd agent reported to date, with a T/N (tumor/normal cell) ratio of up to 23.5 ± 6.6.

Introduction

Gd(III) complexes are extensively used as contrast agents for magnetic resonance imaging (MRI).[1] Recently, there has been a great interest in the development of Gd agents for therapeutic application, in particular binary therapies for the treatment of cancers such as those of the brain.[2] The primary focus of binary therapies is to treat aggressive and intractable cancers whilst minimising toxic side-effects in order to improve patient outcomes. This therapeutic strategy contrasts with traditional cancer therapies, e.g. chemotherapy, which have the detrimental consequence of causing considerable collateral damage to a patient's healthy tissue during the course of

[a]   Dr. D. E. Morrison, Dr. J. B. Aitken, Dr. F. Issa, and Prof. L. M.
       Rendina
       School of Chemistry
       The University of Sydney
       Sydney, NSW 2006 (Australia)
       E-mail: lou.rendina@sydney.edu.au
[b]   Dr. M. D. de Jonge
       X-ray Fluorescence Microscopy beamline
       Australian Synchrotron
       Clayton, Victoria 3168 (Australia)
[c]   Prof. H. H. Harris
       School of Chemistry and Physics
       The University of Adelaide
       Adelaide, SA 5005 (Australia)

       Supporting information for this article is given *via* a link at the end of
       the document.

treatment. Binary therapies endeavor to address these types of issues by means of the combination of two relatively innocuous components which, when combined, allow for a powerful cytotoxic effect to occur *in situ*. In general, binary therapies employ a non-specific, "broad area" component such as neutrons or high-energy X-ray photons and a tumor-specific agent with low cytotoxicity. Of particular interest in this regard are the experimental binary therapies known as neutron capture therapy (NCT)[3] and photon activation therapy (PAT).[4]

NCT combines non-ionising, low-energy (slow) thermal neutron irradiation with suitable nuclides such as the naturally-occurring and non-radioactive ^{10}B or ^{157}Gd isotopes.[2] Both of these nuclides possess very high neutron capture cross-sections which allow for site-specific neutron capture reactions leading to the formation of cytotoxic decay products with a limited range of less than one-cell diameter.[5] In the case of the ^{157}Gd nucleus, the therapeutically-relevant decay products appear to be the Auger and Coster-Krönig (ACK) electrons as they are high linear energy transfer (LET) particles.[5b-e] In contrast, PAT relies on high-energy X-ray photons to instigate the release of photoelectric species including ACK electrons from high-Z elements such as Pt or I which leads to cell death.[6] Synchrotron stereotactic radiotherapy (SSR) is a subset of PAT which incorporates X-ray photons sourced from a synchrotron and tuned at or slightly above the K-edge of the heavy element. Rotation of the patient about the target site in order to increase the relative radiation dose within the tumor site is another feature of SSR.[7] GdSSR (GdPAT) has been proposed as a viable therapy for the treatment of the aggressive and intractable malignant brain tumor known as glioblastoma multiforme,[7] but clinically-suitable Gd agents are yet to be developed.

It has been demonstrated that ACK electrons generated from DNA-bound Gd^{3+} ions have the ability to cleave double-stranded DNA,[8] a direct way of effecting cell death. The lethal effects of ACK electrons are likely due to the subsequent generation of reactive oxygen species (ROs) from water, increasing the oxidative stress within the target cell.[5d, 7] However, ACK electrons possess a mean path length of only *ca.* 12 nm.[9] This extremely short path length imposes another requirement on the design of new Gd-agents for use in binary therapies, i.e. the agents must accumulate within critical sub-cellular organelles such as the nucleus or the mitochondria. Damage to either of these entities can lead to apoptosis.

While there are ever-increasing facilities capable of providing suitable neutron and X-ray sources, there is a dearth of suitable Gd-agents for use in binary therapies such as NCT and PAT. The design of suitable agents for potential use in these binary therapies requires that certain key criteria are met, namely the ability to achieve high tumor selectivity and uptake,

accumulation within critical cellular organelles, and low cytotoxicity in the absence of thermal neutrons or X-ray photons. The first class of compounds to be investigated for use in Gd-based binary therapies were Gd-based contrast agents which are already employed for clinical use in MRI.[5d] However, none of these Gd(III) complexes displayed a significant ability to selectively accumulate within tumor sites nor an ability to localise within important sub-cellular organelles.[5d] DNA-targeted agents have also been investigated in recent years. Two such agents include MGd,[7] **1**, and a Pt(II)-Gd(III) complex **2**.[10] MGd, initially investigated as a chemo- and radio-sensitiser, had been heavily investigated *in vivo* until the FDA ceased further clinical trials with this agent in late 2007.[11] It has been shown that MGd was able to localise within the nuclei of tumor cells.[7] The metallointercalator **2**, was also shown to selectively accumulate within the nuclei of tumor cells *in vitro*.[10] However, the inherent cytotoxicity of DNA-targeted agents such as **2** has hindered further investigation of this class of compounds.
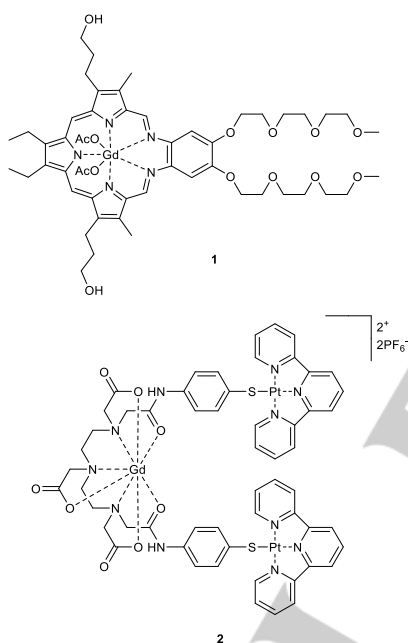
A new avenue for the design of Gd-agents for use in binary therapies includes mitochondria-targeted agents.[12] Delocalised lipophilic cations (DLCs) have garnered increasing attention for their ability to act as tumor-targeted delivery vectors for a range of tumor imaging and therapeutic applications.[13] In particular, tetraphenylphosphonium (TPP) and triphenylmethylphosphonium (TPMP) cations were shown to selectively accumulate in brain tumors with a tumor to normal (T/N) tissue ratio of up to 48 : 1 in a canine brain tumor model.[14] The ability of DLCs to accumulate selectively within the mitochondria of cancer cells stems from the fact that cancer cells typically possess elevated plasma and mitochondria membrane potentials ($\Delta\psi$).[15] For example, the mitochondrial membrane potential of most cancer cells is elevated by 60 mV

when compared to normal, healthy cells. This difference in $\Delta\psi$ promotes the selective uptake of cationic species.

Phosphonium salts have also been implemented extensively in BNCT applications and as PET imaging agents.[13b-g] Their use in the therapeutic delivery of Gd to tumor sites represents a new direction for GdNCT and GdPAT. We recently reported the tumor cell uptake and selectivity of two phosphonium-containing Gd(III) complexes which have set a new benchmark as potential GdNCT and GdPAT agents.[12] Such Gd(III) complexes showed very low *in vitro* cytotoxicity, high tumor uptake and selectivity, and an ability to accumulate within the mitochondria of tumor cells. Indeed, the Gd(III) complexes were able to achieve comparable tumor cell selectivity to the DNA-targeted agents such as **2**, but with far greater tumor uptake and lower cytotoxicity. By means of synchrotron X-ray fluorescence (XRF) quantification, it was demonstrated that that these complexes were able to accumulate Gd at high levels (*ca*. 10^{11} Gd atoms per tumor cell), a few orders of magnitude higher than therapeutically-relevant thresholds.[12]

Herein we report a comprehensive evaluation of selected phosphonium-bearing Gd(III)-agents in an effort to aid in their future design to optimise the key criteria of tumor selectivity, tumor cell uptake, cytotoxicity, and mitochondrial localisation.

Results and Discussion

A primary challenge in the design of mitochondria-targeted Gd(III) complexes is the incorporation of a charged lipophilic species within a Gd(III)-chelator whilst not compromising the high complexation capacity of the chelating agent nor the tumor-targeting ability of the DLC. Ideally, the complex should be monocationic at the phosphonium site and the Gd-macrocycle remains uncharged in order to allow for a selective response to the elevated membrane potentials of cancer cells as well as preserving its ability to cross cell membranes. 1,4,7,10-tetraazacyclododecane-1,4,7-triacetic acid (DO3A) provides a highly suitable scaffold in order to achieve this aim because not only is the DO3A-Gd(III) moiety neutral at physiological pH (7.4),[16] it also provides the strong binding affinity associated with the cyclen-derived polyacetate class of macrocycles and a secondary amine site for further synthetic functionalisation.[17] A triphenylphosphonium moiety can easily be generated from the quaternisation of triarylphosphines by using a standard alkylation reaction. Indeed, coupling the two functional moieties by means of a xylyl linker allows for facile reactions by the use of a dibromoxylene reagent which can undergo nucleophilic substitution reactions involving both triarylphosphines and the secondary amine site of the DO3A macrocycle.

A small library of phosphonium-containing bifunctional Gd(III) complexes was synthesised and characterised in this work. The library consisted of three distinct series of Gd(III) complexes, defined by the nature of the phosphonium cation present. Within each series, the complexes were varied by the substitution pattern of the xylyl group (i.e. *para-, meta- and ortho*-xylyl) linking the phosphonium centre to the DO3A-Gd(III) macrocycle. The different isomers allowed for a variation in intramolecular

distance between the functional moieties, which may have a significant effect on the biological activity of the complexes, in particular their ability to cross cell membranes. The first series of Gd(III) complexes were linked to the parent triphenylphosphonium cation. The second series bore an iodo-functionality in the form of an iodophenyldiphenylphosphonium cation, while the third series contained methoxy substituents in the form of a tris(methoxyphenyl)phosphonium cation. These latter two classes were synthesised in order to modulate the lipophilicity of the complexes to allow for structure-activity relationships (SARs) to be established on the basis of lipophilicity of the phosphonium cation.
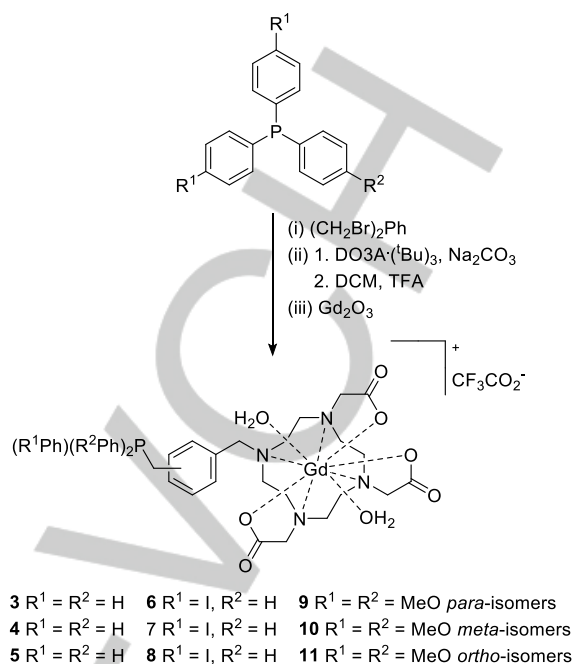
Synthesis

The synthesis of the novel Gd(III) complexes **3** - **11** is summarised in Scheme 1. Commencing from the appropriate triarylphosphine, the dibromoxylene underwent a nucleophilic substitution reaction with the triarylphosphine to give a bromo-xylene functionalised arylphosphonium salt. This reaction was performed in a non-polar solvent (toluene) to promote the precipitation of the monosubstituted species from solution, thus precluding the formation of the undesired disubstituted species. The presence of the bromoxylyl group within the phosphonium salts allowed for facile coupling to a *tert*-butyl protected DO3A macrocycle under basic conditions. Deprotection under acidic conditions using TFA yielded the free ligand in high yield. The ligands were purified by means of reverse-phase HPLC prior to the complexation of Gd^{3+} ions. The complexation reaction was performed by using Gd_2O_3 as this allowed for any excess (insoluble) Gd_2O_3 to be readily removed by means of filtration. The Gd(III) complexes were purified by means of analytical reverse-phase HPLC, with a purity of > 95% achieved for all complexes. The identity of each complex was confirmed by means of high resolution ESI-MS. Through a series of qualitative experiments, the complexes were found to be stable in aqueous media at biologically significant pH following incubation at 37 °C for prolonged periods. Both ESI mass spectrometry and UV-Vis spectroscopy confirmed the robustness of the complexes, even after 24 h in solution.

Determination of lipophilicity

The lipophilicity of DLCs largely governs their ability to traverse and accumulate within tumor-cell mitochondria. Furthermore, lipophilicity plays an important role in the absorption, distribution, metabolism and excretion of therapeutic compounds, and so the lipophilicity of the prepared complexes was used as the basis for determining structure-activity relationships (SARs) of the novel Gd(III) complexes. Log*P* values were determined for the Gd(III) complexes **3** - **11**, as well as the parent triarylphosphonium salts TPP, TPMP and ITPMP, by using a reverse-phase HPLC method involving standard reference compounds. A summary of results is shown in Table 1.

The log*P* values determined for the Gd(III) complexes were comparable to those of the simple phosphonium cations, indicating that the inclusion of the DO3A macrocycle does not greatly impact on the overall lipophilicity of the Gd(III) complexes. Structural variation of the phosphonium cation resulted in the

3 $R^1 = R^2 = H$ **6** $R^1 = I, R^2 = H$ **9** $R^1 = R^2 = MeO$ *para*-isomers
4 $R^1 = R^2 = H$ **7** $R^1 = I, R^2 = H$ **10** $R^1 = R^2 = MeO$ *meta*-isomers
5 $R^1 = R^2 = H$ **8** $R^1 = I, R^2 = H$ **11** $R^1 = R^2 = MeO$ *ortho*-isomers

Scheme 1: Synthesis of phosphonium-containing Gd(III) complexes

observed trend for lipophilicity being trismethoxy-bearing > iodo-bearing > parent phosphonium complexes. The experimental log*P* values were consistent with the observed aqueous solubility of the complexes, where both the parent and the iodo-parent analogue were soluble at levels > 20 mg/mL, while the methoxy-bearing analogue was only found to be soluble at *ca*. 10 mg/mL. Isomeric variations pertaining to the xylyl linker used within the Gd(III) complexes resulted in the observed trend for lipophilicity being *ortho* > *meta* > *para*. This trend indicates that the greater the spatial separation of the two functional moieties, the lower the overall lipophilicity of the complexes. This is likely to be related to the increase in the overall dipole moment of the complexes in the order *ortho* < *meta* < *para*.

In vitro cytotoxicity studies

In vitro cytotoxicities were determined by means of standard MTT colourimetric assays. Assays were performed up to 500 *µ*M of Gd(III) complex. The maximum concentration used in these experiments exceeded the expected dosing concentrations for subsequent *in vitro* and *in vivo* testing. At this maximum concentration, cell viability was not reduced below 50% by any of the Gd(III) complexes. However the cell viability at the maximum concentrations were determined and used as the basis for comparing cytotoxicities (Table 2). Statistical analyses, by means of a two-tailed Student's *t*-test with an *α* value of 0.05, were performed in order to ascertain which differences in cell viability as a result from treatment with the Gd(III) complexes were significant. The only instances where cell viability did not differ significantly from the control cells following treatment were for complexes **3** and **4**. As cell viability correlates inversely with

Table 1. Experimental log$P$ values for Gd(III) complexes and phosphonium cations.

Compound	log$P$[a]
3	1.24 ± 0.02
4	1.35 ± 0.02
5	1.56 ± 0.02
6	1.44 ± 0.03
7	1.53 ± 0.01
8	2.09 ± 0.03
9	1.86 ± 0.08
10	1.91 ± 0.01
11	2.73 ± 0.01
TPP	1.20 ± 0.01
TPMP	0.72 ± 0.02
ITPMP	1.47 ± 0.01

[a] Mean ± SE

Table 2. Mean cell viability of T98G cells treated with 500 μM of Gd(III) complexes for 72 h.

Compound	%Viability[a]	N
3	97 ± 3%	9
4	101 ± 4%	9
5	85 ± 2%	9
6	85 ± 3%	9
7	60 ± 3%	9
8	65 ± 4%	9
9	89 ± 4%	9
10	90 ± 2%	9
11	87 ± 2%	9

[a] Mean ± SE

Table 3. IC$_{50}$ values for complexes **3**, **6** and **9** in the T98G cell line.

Compound	IC$_{50}$ (mM)[a]	N
3	2.55 ± 0.33	4
6	2.14 ± 0.32	4
9	1.42 ± 0.20	4

[a] Mean ± SE

cytotoxicity, preliminary trends for *in vitro* cytotoxicity could thus be determined.

In the parent series, complexes **3** and **4** exhibited a lower cytotoxicity than complex **5**. For the iodo-bearing series, complex **6** exhibited lower cytotoxicity than complexes **7** and **8**. No significant difference was observed between complexes **7** and **8**. For the methoxy-bearing series, there was no observed difference between the three complexes **9** - **11**. This gives a general trend that increased lipophilicity due to decreasing the distance between the functional moieties led to either a comparable or higher cytotoxicity.

Comparing the different sets of compounds with similar xylyl isomers, complex **3** was found to be less cytotoxic than **6**. Complex **9** was not found to be significantly different from either complex **3** or **6**. Complex **4** was the least cytotoxic of the *meta*-xylyl bearing complexes, followed by **10**, with **7** found to be the most cytotoxic. Complexes **5** and **11** did not show any significant difference between cytotoxicity and were both less cytotoxic than **8**. The effect of the inclusion of the iodo functionality into the phosphonium cation led to a clear increase in cytotoxicity in all cases. However, the effect of inclusion of methoxy-substituents was less clear. Indeed, due to the lack of any statistically significant differences, general trends cannot be drawn from these comparisons.

For the parent series and the iodo-bearing series, it was found that an increase in lipophilicity led to comparable or higher cytotoxicities. This trend was not observed for the methoxy-bearing series and may indicate that these species behave

differently within cells to the parent and iodo-bearing series. Indeed, previously reported synchrotron X-ray fluorescence (XRF) elemental mapping has shown a significant difference between the cellular localisation of the iodo-series and the methoxy-series.[12]

In order to further probe the *in vitro* cytotoxicity of the complexes, higher concentrations of Gd(III) complex were used (up to a final concentration of 4 mM). IC$_{50}$ values are reported in Table 3. The IC$_{50}$ values agree with previously obtained trends for cytotoxicity by means of cell viability at 500 μM. (*vide supra*).

In vitro uptake studies on whole cells

In vitro cellular uptake studies were performed with complexes **3**, **6** and **9** in the T98G cell line and primary human carotid artery endothelial cells (HCtAEC). Cells were incubated in the presence of 100 μM of Gd(III) complex for 48 h, prior to cell harvesting and analysis by means of ICP-MS. All three of the complexes showed significantly greater uptake into the T98G

tumor cell line compared to the HCtAEC normal cells. Tables 4 and 5 provide a summary of Gd uptake into the tumor and normal cell lines expressed in terms of ng of Gd per mg of protein, respectively.

The ratio of tumor to normal uptake (T/N) provides an indication of *in vitro* selectivity of the complexes. Complex **3** showed the highest T/N selectivity at 23.5 ± 6.6, while complexes **6** and **7** exhibited T/N selectivities of 7.7 ± 1.6 and 6.0 ± 1.8, respectively. The significantly greater selectivity of complex **3** is likely due to its lower relative uptake into the normal cell line compared to **6** and **9**. All three complexes showed comparable uptake into tumor cells under the conditions of the experiment.

The observed uptake and selectivity results for the complexes indicate that a higher lipophilicity is not a necessary requirement for significant uptake into tumor cells whilst increased lipophilicity can lead to greater uptake into normal cells leading to a decrease in overall selectivity and a potentially lowered effectiveness of the Gd agent.

in the presence of 100 μM of Gd(III) complex for 48 h prior to cell harvesting and then subjected to a reagent-based mitochondria isolation kit. The fractions for the pure mitochondria and the cytosol were collected and analysed by means of ICP-MS for Gd content. All three complexes showed Gd accumulated into the mitochondria. Results for mitochondrial selectivity are reported in terms of the ratio of the mitochondrial to cytosolic fractions (M/C) (Table 6).

Complex **9** showed the highest mitochondrial selectivity with an M/C ratio of 5.4 ± 2.4, while complexes **3** and **6** had M/C ratios of 2.0 ± 0.6 and 3.4 ± 2.3 respectively. These results indicate that, as expected, increased lipophilicity allows for greater mitochondrial accumulation. When the M/C ratios are considered along with the results for tumor uptake and selectivity it is clear that overall lipophilicity is an important tuneable property for maximising tumor uptake and mitochondrial accumulation of phosphonium-bearing Gd-DO3A complexes.

Table 4. ICP-MS analysis of Gd in T98G tumor cells treated with **3**, **6** and **9** (100 μM) for 48 h, expressed as ng Gd/mg of protein.

	Control	**3**	**6**	**9**
Mean	0.53	4071.6	5355.0	4824.4
SE	0.11	605.8	124.7	1006.8
N	3	3	3	3
Sig. Different (Y/N)[a]	N/A	Y	Y	Y

[a] Statistical significance was accepted at the 95% confidence interval with *p*-values determined using the Mann-Whitney U test.

Table 6. ICP-MS analysis of Gd in T98G cells treated with **3**, **6** and **9** (100 μM) for 48 h, expressed as a ratio of Gd content in the mitochondrial fraction compared to the cytosolic fraction.

	Control	**3**	**6**	**9**
Mean	0.5	2.0	3.4	5.4
SE	0.3	0.6	2.3	2.4
N	4	4	4	4

Synchrotron X-ray Fluorescence (XRF) Studies
T98G Human Glioblastoma Cell Line

Synchrotron X-Ray fluorescence (XRF) studies were performed on T98G tumor cells treated with selected Gd(III) complexes to allow for visualisation of elemental distribution within individual cells. Data were collected for control cells and cells treated with 100 μM of complexes **3**, **6** and **7** for 24 h. Cells were grown on Si$_3$N$_4$ windows and fixed using MeOH at -78 °C.

Figures 1 - 3 show elemental maps of a single T98G cell incubated with 100 μM of **3**, **6** and **7** for 24 h, respectively. XRF quantitation of intracellular Gd content is summarized in Table 7. Statistically significant (single-tailed Mann-Whitney U test, $p < 0.05$) levels of Gd were present in the cells after treatment with all of the complexes. For all three complexes, the synchrotron XRF elemental density maps for Gd showed a strong correlation to regions of high intensity in the Fe elemental density maps. This elemental correlation is consistent with mitochondrial uptake of the complexes due to the key role the mitochondria play in cellular Fe regulation, metabolism (e.g. heme synthesis and Fe–S cluster assembly), and storage due to mitochondrial ferritin (MtFe).[18] Quantified intracellular content of Gd within the cells following treatment with **3**, **6** and **7** exhibited a positive correlation with lipophilicity.
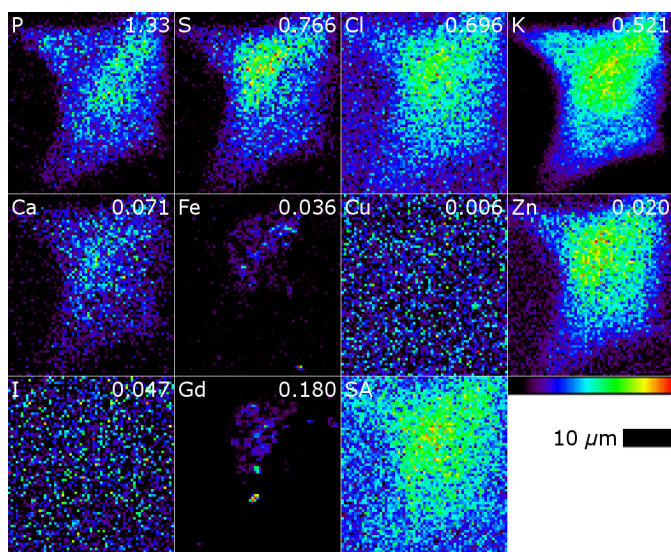
Table 5. ICP-MS analysis of Gd in HCtAEC cells treated with **3**, **6** and **9** (100 μM) for 48 h, expressed as ng Gd/mg of protein.

	Control	**3**	**6**	**9**
Mean	0.05	173.3	697.9	803.7
SE	0.05	41.0	144.1	168.1
N	3	4	3	4
Sig. Different (Y/N)[a]	N/A	Y	Y	Y

[a] Statistical significance was accepted at the 95% confidence interval with *p*-values determined using the Mann-Whitney U test.

In vitro mitochondria uptake studies

In vitro mitochondria uptake studies were performed with complexes **3**, **6** and **9** in the T98G cell line. Cells were incubated
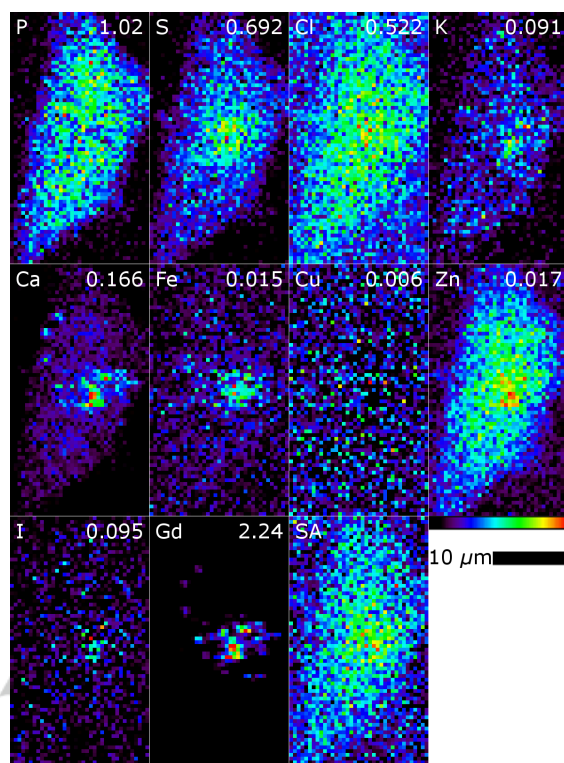
Figure 1: Scattered X-ray (SA) and XRF elemental distribution maps showing P, S, Cl, K, Ca, Fe, Cu, Zn, I and Gd for the T98G Cell C treated with 100 μM of **3** for 24 h.
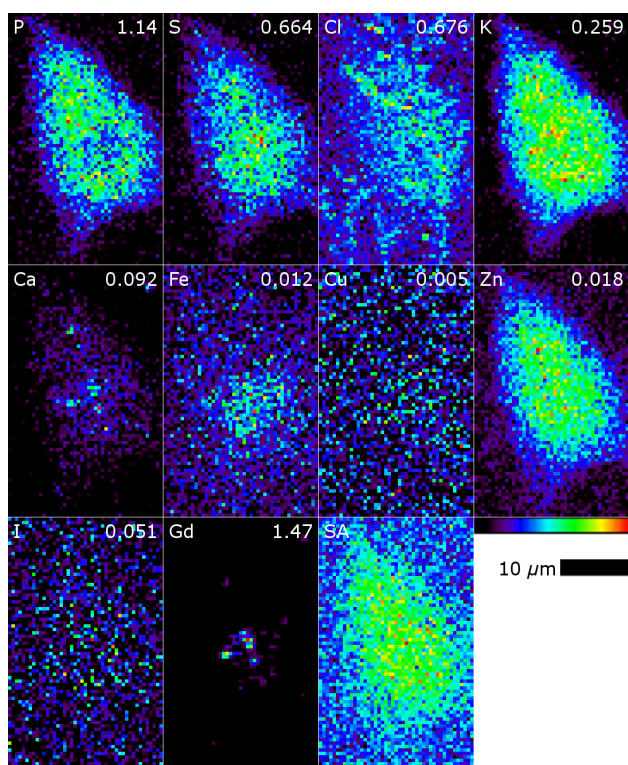

Figure 2: Scattered X-ray (SA) and XRF elemental distribution maps showing P, S, Cl, K, Ca, Fe, Cu, Zn, I and Gd for the T98G Cell A treated with 100 μM of **6** for 24 h.

Figure 3: Scattered X-ray (SA) and XRF elemental distribution maps showing P, S, Cl, K, Ca, Fe, Cu, Zn, I and Gd for the T98G Cell D treated with 100 µM of **7** for 24 h.

Table 7. Mean Gd uptake within individual T98G human glioblastoma cells following treatment with complexes **3**, **6** and **7**, as determined by synchrotron X-ray fluorescence (XRF) imaging.

Complex	Incubation Time (h)	Gd density /cell[a]	N
3	24	0.004 ± 0.002	5
6	24	0.06 ± 0.04	5
7	24	0.12 ± 0.05	5

[a] Mean ± SD in μg cm^{-2}.

A549 Human Lung Cancer Cell Line

Synchrotron X-Ray fluorescence (XRF) studies were performed on A549 tumor cells treated with selected Gd(III) complexes to allow for visualisation of elemental distribution within individual cells. Data were collected for control cells and cells treated with 100 μM of complexes **3** and **6** for 24 h. Cells were grown on Si$_3$N$_4$ windows and fixed using MeOH at -78 °C. For comparison, additional cells treated with **6** were fixed by means of flash freezing in a liquid N$_2$/*iso*-pentane slurry.

Figures 4 and 5 show elemental maps of a single A549 cell incubated with 100 μM of **3** and **6,** respectively, for 24 h and then fixed in MeOH. Figure 6 shows elemental maps of a single A549 cell incubated with **6** for 24 h and fixed by flash freezing. XRF quantitation of intracellular Gd content is summarized in Table 8. Statistically significant (single-tailed Mann-Whitney U test, $p < 0.05$) levels of Gd were present in the cells after treatment with all of the complexes. For all three cases, the synchrotron XRF elemental density maps for Gd showed a strong correlation to regions of high intensity in the Fe elemental density maps. This observation agrees with the observations made for the XRF experiments performed using the T98G cell line (*vide supra*), supporting the hypothesis of mitochondrial localisation. Similarly, the difference in uptake of **3** and **6** were positively correlated to lipophilicity.
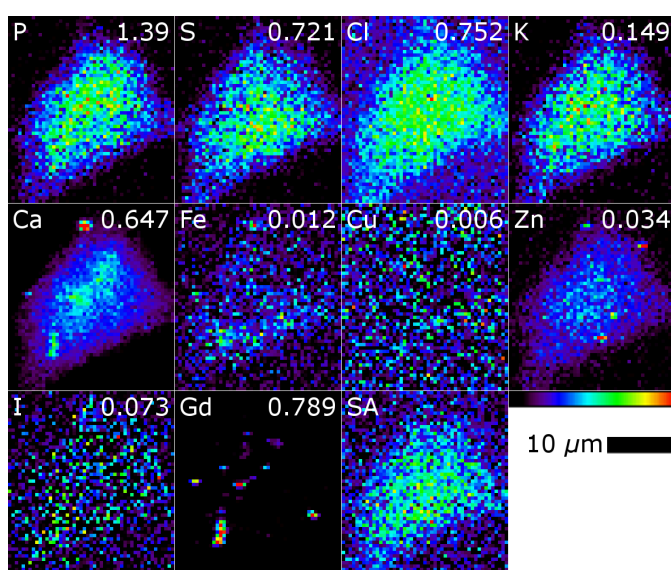
Table 8. Mean Gd uptake within individual A549 human lung cancer cells following treatment with complexes **3** and **6**, as determined by synchrotron X-ray fluorescence (XRF) imaging.

Complex	Incubation Time (h)	Gd density /cell[a]	N
3[b]	24	0.010 ± 0.009	2
6[b]	24	0.05 ± 0.03	5
6[c]	24	0.02 ± 0.01	5

[a] Mean ± SD in μg cm^{-2}. [b] Fixed by using MeOH at -78°C. [c] Fixed by flash freezing in a liquid N_2/*iso*-pentane slurry.

Figure 4: Scattered X-ray (SA) and XRF elemental distribution maps showing P, S, Cl, K, Ca, Fe, Cu, Zn, I and Gd for the A549 Cell A treated with 100 μM of **3** for 24 h.

Figure 5: Scattered X-ray (SA) and XRF elemental distribution maps showing P, S, Cl, K, Ca, Fe, Cu, Zn, I and Gd for the A549 Cell B treated with 100 μM of **6** for 24 h.
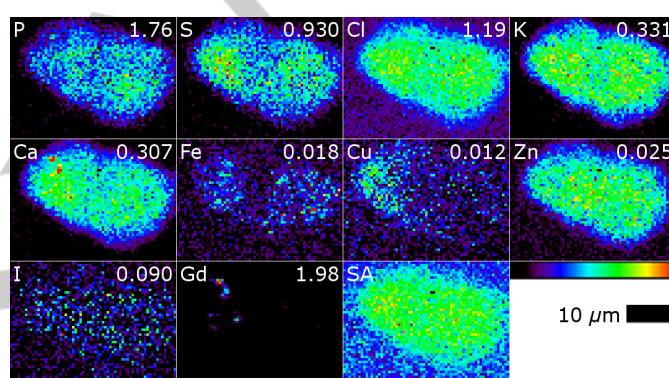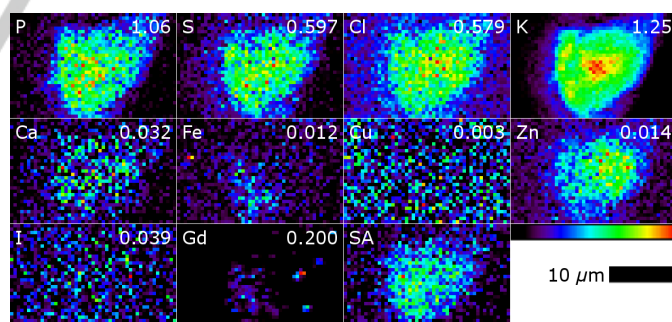

Figure 6: Scattered X-ray (SA) and XRF elemental distribution maps showing P, S, Cl, K, Ca, Fe, Cu, Zn, I and Gd for the A549 Cell B treated with 100 μM of **6** for 24 h and fixed by flash freezing in a liquid N_2/iso-pentane slurry.

The difference in Gd uptake observed for **6,** when the means of fixation were varied, highlights the effect of elemental leaching during the fixation process and the importance of selection of an appropriate protocol to minimise this effect. Flash freezing in a slurry of liquid N_2/*iso*-pentane appears to have a more profound effect on the leaching of Gd compared to fixation in MeOH at -78°C. Studies that used formaldehyde for fixation showed higher Gd uptake in T98G cells in comparison to the values reported here, lending to the hypothesis that less Gd is leached from the cells during fixation with formaldehyde compared to MeOH or flash freezing.[12] Alternatively, variations may arise from differences in uptake between cells in different phases.

Conclusions

A library of new Gd(III) complexes **3** – **11** was shown to address many key criteria for the development of new therapeutic PAT and NCT agents. All complexes were found to be essentially non-cytotoxic at the expected therapeutically-relevant concentrations. They were also shown to selectively accumulate within tumor cells more effectively than normal cells and achieve excellent mitochondrial localisation. Lipophilicity appears to play a major role in the cytotoxicity, uptake and selectivity of this class of phosphonium-bearing complexes. Of particular interest, the parent complex **3** exhibited a T/N ratio of 23.5 ± 6.6, a value which was 3 - 4 times greater than the substituted derivatives **6** and **9**. Indeed, this selectivity value exceeds those previously determined for clinical agents such as MGd.

The series of complexes containing the tris(methoxyphenyl)phosphonium cation exhibited differing behaviour compared to the parent and iodophenyldiphenylphosphonium series. In the parent and iodinated series, lipophilicity correlated well with increased cytotoxicity. However, for the methoxy-bearing series, lipophilicity did not strongly correlate with cytotoxicity. Coupled with the significant difference in the biological behaviour of the methoxy-bearing complexes, we hypothesise that these complexes may undergo a different mechanism of uptake or mode of action within the cell compared to the parent or iodo-bearing complexes. Further experiments are required to understand the apparent differences in biological behaviour between these classes of complexes.

There were key differences found in the observed trends for Gd uptake correlated to lipophilicity between the ICP-MS studies and the XRF studies. These differences are likely to arise from the differences in experimental conditions, e.g. the cell growth density, the incubation times, and the treatment of the cells post incubation; however, further work is required to unravel the factors involved. Notably, the ICP-MS studies indicate that lipophilicity may play a role in the ability of the Gd(III) complexes to be taken up into normal, healthy cells. This factor alone led to significant differences in the observed *in vitro* tumor selectivity of the complexes. Additionally, mitochondrial isolation studies indicate that an increased lipophilicity can lead to enhanced mitochondrial localisation of the Gd(III) complexes.

Taken together, the *in vitro* cytotoxicity and whole cell uptake studies demonstrate that an increased lipophilicity of the Gd(III) complexes prepared in this work can lead to a somewhat increased cytotoxicity and a decreased tumor cell selectivity. However, this observation must be tempered against the enhanced mitochondrial localisation that any increased lipophilicity might bring. However, it is clear from this study that a delicate balance exists between lipophilicity, cytotoxicity, tumor cell selectivity, and mitochondrial localisation, and all these properties must be considered in the design of new phosphonium-based Gd-agents for potential use in binary therapies such as GdNCT and GdPAT. Furthermore, *in vivo* data are required to confirm the observed *in vitro* trends and such studies will be conducted in due course.

Experimental Section

General

All reactions were performed under a dry N_2 atmosphere where required. All manipulations were performed by using conventional Schlenk techniques.[19]

Instrumentation

All ^{1}H, ^{13}C{^{1}H}, ^{19}F{^{1}H} ^{31}P{^{1}H} NMR spectra were recorded at 300 K on a Bruker Avance300 spectrometer (^{1}H at 300 MHz, ^{13}C at 75 MHz, ^{19}F at 282 MHz, and ^{31}P at 121 MHz). All NMR signals (δ) are reported in ppm. ^{1}H and ^{13}C{^{1}H} NMR spectra were referenced according to their solvent residual peaks. ^{31}P{^{1}H} NMR spectra were referenced to external $P(OMe)_3$ at 140.85 ppm. Relaxivity measurements were recorded on a Bruker Minispec mq60 spectrometer at 60 MHz. UV-Visible spectra were recorded on a Thermo Scientific Nanodrop 2000 UV-Vis spectrophotometer. Low resolution ESI-MS were recorded on a Finnigan LCQ mass spectrometer. High resolution ESI-FT-ICR-MS data was recorded on a Bruker 7.0T mass spectrometer. Melting points were recorded on a Barnstead Electrothermal IA9100 digital melting point apparatus. Values reported are uncorrected.

HPLC Methods

Method 1 - Preparative

Performed on a Waters 600 HPLC system with a Waters 486 tuneable absorbance UV/vis detector (λ = 254 nm) and a Sunfire C18 preparative column (19 × 150 mm, 5 μm pore size). Flow rate 7 ml/min. HPLC was performed under gradient flow conditions, commencing with 95% Solvent A (0.1% trifluoroacetic acid in water) and 5% Solvent B (0.1% trifluoroacetic acid in acetonitrile) and moving to 20% Solvent A and 80% Solvent B over 30 min.

Method 2 - Analytical

Performed on a Waters 2965 separation module HPLC system with a Waters 2996 photodiode array (PDA) detector (λ = 200 to 300 nm) and a Sunfire C18 analytical column (2.1 × 150 mm, 5 μm pore size). Flow rate 0.2 ml/min. HPLC was performed under gradient flow conditions, commencing with 95% Solvent A (water) and 5% Solvent B (acetonitrile) going to 0% Solvent A and 100% Solvent B over 15 min.

Materials and Methods

Distilled water was used for all experiments requiring water. MeCN, and PhMe were dried prior to use according to Armarego and Chai.[20] MeCN was freshly distilled from CaH_2 before use. PhMe was dried over sodium wire and freshly distilled prior to use. All other solvents were used without prior preparation.

All precursor chemicals used in this study were commercially available. Triethylenetetraamine was purchased from Alfa Aeser. All other reagents were purchased from the Sigma Aldrich Chemical Co.

Cyclen was prepared by methods previously described by Athey *et al.*[21] DO3A-^{t}Bu$_3$·HBr was prepared as previously described by Moore.[22]

Synthesis of precursors and ligand intermediates are detailed in the Supporting Information.

Gd(III) Complexes

General procedure

The free bifunctional ligands **L1**-**L9** were stirred as a suspension with Gd_2O_3 (2 equiv.) in H_2O at 80 °C for 12 h (or until completion). The mixture was then centrifuged and filtered off to remove unreacted and insoluble Gd_2O_3. The filtrate was then reduced *in vacuo* and the product lyophilised to give a white powder. The purity of the complex was confirmed by means of analytical reverse-phase HPLC (Method 2).

The hydration state, *q*, of Gd(III) complexes can be inferred from correlation of the longitudinal relaxivity, r_1, with similarly structured Gd(III) complexes with known hydration states.[23] The relaxivity of complexes **3**, **6** and **9** were measured as 5.1, 9.6 and 7.4 mM^{-1} s^{-1}, respectively. Gd-DOTA has a relaxivity of 3.6 mM^{-1} s^{-1} and the *N*-substituted DO3A derivative Gadoteridol has a relaxivity of 4.1 mM^{-1} s^{-1}.[24] Both Gd-DOTA and Gadoteridol possess a hydration state of 1.[24] The relatively higher relaxivities of **6** and **9** suggest a hydration state of 2, while the lower relaxivity of **3** suggests a hydration state of 1. The hydration states of the *m*- and *o*-isomer complexes were approximated from the values determined for the *p*-isomer complexes.

Stability in aqueous media was observed over a range of pH 6 to 7.4 by two separate methods. In method 1, solutions of the complexes were prepared in acetate buffer (pH 6) in the presence of bovine serum albumin (BSA) using Xylenol Orange as an indicator and incubated at 37 °C with periodic recording of UV-Visible spectra. No change was observed in the spectra over 24 hours. In a comparison experiment using $GdCl_3$, a distinct shift in λ_{max} was observed after 6 h of incubation.

In method 2, solutions of the complexes were prepared in phosphate buffered saline (PBS, pH 7.4) and incubated at 37 °C for 24 h and observed by mean of ESI-mass spectrometry. The signals with *m/z* corresponding to the [M–CF_3CO_2]$^+$ of the complexes were observed with no evidence for the presence of free ligand or other complex species.

2,2',2''-(10-(4-((Triphenylphosphonio)methyl)benzyl-1,4,7,10-tetraazacyclododecane-1,4,7-triyl)triacetatogadolinium(III) trifluoroacetate (3)

The reaction was performed using **L1** (79.5 mg, 96.4 *μ*mol) and Gd_2O_3 (39.7 mg, 110 *μ*mol). Yield 73.1 mg (77.5 %). t_R = 11.6 min. Purity > 95% by HPLC. M.p. > 300 °C (decomp.). ESI-FT-ICR-MS for [M–CF_3CO_2 + H]$^{2+}$: Calculated *m/z* 433.6196; Found 433.6196.

2,2',2''-(10-(3-((Triphenylphosphonio)methyl)benzyl-1,4,7,10-tetraazacyclododecane-1,4,7-triyl)triacetatogadolinium(III) trifluoroacetate (4)

The reaction was performed using **L2** (57.8 mg, 70.1 *μ*mol) and Gd_2O_3 (27.0 mg, 74.5 *μ*mol). Yield 53.4 mg (76.1 %). t_R = 13.8 min. Purity > 95% by HPLC. M.p. > 300 °C (decomp.). ESI-FT-ICR-MS for [M–CF_3CO_2 + H]$^{2+}$: Calculated *m/z* 433.6196; Found 433.6196.

2,2',2''-(10-(2-((Triphenylphosphonio)methyl)benzyl-1,4,7,10-tetraazacyclododecane-1,4,7-triyl)triacetatogadolinium(III) trifluoroacetate (5)

The reaction was performed using **L3** (46.9 mg, 56.9 *μ*mol) and Gd_2O_3 (11.1 mg, 30.7 *μ*mol). Yield 44.2 mg (79.3 %). t_R = 14.8 min. Purity > 95%

by HPLC. M.p. > 280 °C (decomp.). ESI-FT-ICR-MS for [M–CF_3CO_2]$^+$: Calculated *m/z* 866.2322; Found 866.2322.

2,2',2''-(10-(4-(((4-Iodophenyl)diphenylphosphonio)methyl)benzyl)-1,4,7,10-tetraazacyclododecane-1,4,7-triyl)triacetatogadolinium(III) trifluoroacetate (6)

The reaction was performed using **L4** (59.0 mg, 62.0 *μ*mol) and Gd_2O_3 (12.8 mg, 35.3 *μ*mol). Yield 48.1 mg (70.2 %). t_R = 11.8 min. Purity > 95% by HPLC. M.p. > 270 °C (decomp.). ESI-FT-ICR-MS for [M–CF_3CO_2]$^+$: Calculated *m/z* 992.1285; Found 992.1291.

2,2',2''-(10-(3-(((4-Iodophenyl)diphenylphosphonio)methyl)benzyl)-1,4,7,10-tetraazacyclododecane-1,4,7-triyl)triacetatogadolinium(III) trifluoroacetate (7)

The reaction was performed using **L5** (61.9 mg, 65.1 *μ*mol) and Gd_2O_3 (13.7 mg, 37.7 *μ*mol). Yield 49.0 mg (68.1 %). t_R = 13.5 min. Purity > 95% by HPLC. M.p. > 270 °C (decomp.). ESI-FT-ICR-MS for [M–CF_3CO_2]$^+$: Calculated *m/z* 992.1285; Found 992.1326.

2,2',2''-(10-(2-(((4-Iodophenyl)diphenylphosphonio)methyl)benzyl)-1,4,7,10-tetraazacyclododecane-1,4,7-triyl)triacetatogadolinium(III) trifluoroacetate (8)

The reaction was performed using **L6** (107.6 mg, 113 *μ*mol) and Gd_2O_3 (43.7 mg, 12.1 *μ*mol). Yield 65.5 mg (52.4 %). t_R = 18.4 min. Purity > 95% by HPLC. M.p. > 250 °C (decomp.). ESI-FT-ICR-MS for [M–CF_3CO_2]$^+$: Calculated *m/z* 992.1285; Found 992.1289.

2,2',2''-(10-(4-((Tris(4-methoxyphenyl)phosphonio)methyl)benzyl)-1,4,7,10-tetraazacyclododecane-1,4,7-triyl)triacetatogadolinium(III) trifluoroacetate (9)

The reaction was performed using **L7** (98.8 mg, 108 *μ*mol), and Gd_2O_3 (47.5 mg, 131 *μ*mol). Yield 94.8 mg (81.5%). t_R = 14.7 min. Purity > 95% by HPLC. M.p. > 300 °C (decomp.). ESI-FT-ICR-MS for [M–CF_3CO_2]$^+$: Calculated *m/z* 956.2636; Found 956.2646.

2,2',2''-(10-(3-((Tris(4-methoxyphenyl)phosphonio)methyl)benzyl)-1,4,7,10-tetraazacyclododecane-1,4,7-triyl)triacetatogadolinium(III) trifluoroacetate (10)

The reaction was performed using **L8** (46.5 mg, 50.8 *μ*mol), and Gd_2O_3 (62.77 mg, 173 *μ*mol). Yield 52.2 mg (96.0%). t_R = 11.5 min. Purity > 95% by HPLC. M.p. > 300 °C (decomp.). ESI-FT-ICR-MS for ([M–CF_3CO_2]$^+$)$_3$: Calculated *m/z* 955.9307; Found 955.9320.

2,2',2''-(10-(2-((Tris(4-methoxyphenyl)phosphonio)methyl)benzyl)-1,4,7,10-tetraazacyclododecane-1,4,7-triyl)triacetatogadolinium(III) trifluoroacetate (11)

The reaction was performed using **L9** (126.5 mg, 138 *μ*mol), and Gd_2O_3 (234.76 mg, 648 *μ*mol). Yield 144.3 mg (97.7%). t_R = 11.5 min. Purity > 95% by HPLC. M.p. > 300 °C (decomp.). ESI-FT-ICR-MS for [M–CF_3CO_2]$^+$: Calculated *m/z* 956.2639; Found 956.2629.

Determination of Log*P* values by a HPLC method

The log*P* values of complexes **3**-**11** were measured using a standard reverse phase HPLC method. Phosphate buffer (0.05 M) was prepared by dissolving KH_2PO_4 (3.4 g, 25 mmol) in H_2O (500 mL) and the pH was

adjusted to *ca.* 7 with NaOH solution (0.1 M). Samples were analysed using a Waters Sunfire C18 column (2.1 × 150 mm) with a mobile phase of MeOH and phosphate buffer (65:35 *v/v*) with a flow rate of 0.2 mL/min, UV absorbance at 254 nm. The lipophilicity of each compound was calculated by comparison of its retention time to that of known standards. The standard curve was generated using acetone, 2-butanone, aniline, toluene, diphenylamine, triphenylamine, and hexachlorobenzene. Samples were prepared at a concentration of 1 mg/mL in MeOH. Retention times were collected in duplicate. Retention times were adjusted for the T_0, and a standard curve plotting log*P vs.* retention time was generated (y = $0.5368e^{0.8991x}$; r^2 = 0.9949).

Biological Assays

In vitro cytotoxicity and cell uptake studies

Human glioblastoma multiforme (T98G) cells were maintained as monolayers in minimum essential medium supplemented with 10% fetal bovine serum, penicillin (100 units/mL), streptomycin (100 μg/mL) and L-glutamine (2.5 mM), at 37 °C in a humified 5% CO_2 atmosphere. Primary human carotid artery endothelial cells (HCtAEC) were harvested from normal carotid arteries and obtained commercially (Cell Applications, Inc, SD). Where required, HCtAECs were cultured in complete media comprising MesoEndo Cell Growth Medium (Cell applications, SD), fetal bovine serum (10% *v/v*), 2 mM L-glutamine, 100 units/mL penicillin, 100 μg/mL streptomycin, and 15 μg/mL endothelial cell growth supplement (Millipore, Sydney, Australia) at 37°C under 5% CO_2.

Cytotoxicity assays

The cytotoxicity of complexes was assessed using the 3-(4,5-dimethylthiazol-2-yl)-2,5-diphenyltetrazolium bromide (MTT) assay.[25] Briefly, cells were harvested with trypsin (0.1% *v/v*), and cell pellets were isolated by centrifugation. Cells were then re-suspended to a single cell suspension, cell numbers were counted using a hemocytometer (Weber), and then cells were seeded (density 1 × 10^4 cells per well) in growth medium (100 μL) using 96-well plates and were allowed to adhere overnight at 37 °C. Cells were incubated at 37 °C in a humified atmosphere of 5% CO_2 in the presence of complexes **3-11** or the vehicle (control). Serial dilutions of the Gd complex were added to triplicate or duplicate wells. Maximum concentration (MaxC) for the experiments were either 500 μM (*N* = 9) or 4 mM (*N* = 4). After 72 h, MTT solution in phosphate-buffered saline (PBS; 30 μL, 0.17% *w/v*) was added and the incubation was continued. After a further 4 h, the culture medium and excess MTT solution were removed and the resulting MTT–formazan crystals dissolved by addition of 150 μL DMSO. Cell viability was determined by measuring the absorbance at either 600 nm using a Victor3V microplate reader (PerkinElmer). All readings were corrected for absorbance from wells containing the vehicle alone, and the level of MTT was expressed relative to the corresponding vehicle-treated controls as % viability. Corresponding IC_{50} values for each of the compounds tested were then determined at the dose required to induce a 50% decrease in cell viability. All experiments were conducted at least in triplicate and all IC_{50} values are reported with standard errors where possible.

Cell uptake studies

Stock solutions of **3** and **6** (20 mM in H_2O) and **9** (10 mM in H_2O) were prepared. Warm (37 °C) culture medium was treated with the stock Gd solutions to a final concentration of 100 μM. The T98G cells were cultured as a monolayer in 25-cm^2 flasks to 70–80% confluence and then incubated with the Gd-containing culture medium at 100 μM for 48 h at

37 °C in a humidified 5% CO_2 atmosphere. The medium was removed and the cells were washed once with PBS (1 mL). PBS (2 mL) was added to the culture flask and then cells were harvested with a rubber policeman. Harvested cells were sedimented by centrifugation at 3000 rpm for 5 min, and then the supernatant removed. PBS (2 mL) was added to the cell pellet, which was then pipetted until a single cell suspension was achieved. An aliquot (100 μL) was taken for protein analysis. The remaining cells were sedimented by centrifugation at 3000 rpm for 5 min, then the supernatant was removed and the cell pellet was analysed for Gd content by means of ICP-MS.

The HCtAEC cells were cultured as a monolayer in 6 well plates to 70-80% confluence and then incubated with the Gd-containing culture medium at 100 μM for 48 h at 37 °C in a humidified 5% CO_2 atmosphere. The medium was removed and the cells were washed once with PBS (1 mL). Cells were harvested with trypsin (1 mL, 0.1% *v/v*) for 5 minutes at 37 °C, and then media (1 mL) was added. Harvested cells were sedimented by centrifugation at 3000 rpm for 5 min, and then the supernatant removed. PBS (1 mL) was added to the cell pellet, which was then pipetted until a single cell suspension was achieved. The cells were re-sedimented by centrifugation. PBS (2 mL) was added to the cell pellet, which was then pipetted until a single cell suspension was achieved. An aliquot (100 μL) was taken for protein analysis. The remaining cells were sedimented by centrifugation at 3000 rpm for 5 min, then the supernatant was removed and the cell pellet was analysed for Gd content by means of ICP-MS.

Cell pellets were digested in HNO_3 (0.5 mL, 69%) at 65 °C in a water bath for 18 h. The digest was diluted to 10 mL with HCl (0.1 M), and then measured for Gd by means of ICP-MS. ICP-MS was run on a Perkin Elmer ELAN 6100 Inductively Coupled Plasma Emission Mass Spectrometer (ICP-MS) at the Solid State and Elemental Analysis Unit (UNSW Analytical Centre). Gd uptake concentrations are reported as ng Gd/mg protein.

Mitochondria isolation studies

Stock solutions of **3** and **6** (20 mM in H_2O) and **9** (10 mM in H_2O) were prepared. Warm (37 °C) culture medium was treated with the stock Gd solutions to a final concentration of 100 μM. The T98G cells were cultured as a monolayer in 75-cm^2 flasks to 70–80% confluence and then incubated with the Gd-containing culture medium at 100 μM (treated) or with untreated culture medium (control) for 48 h at 37 °C in a humidified 5% CO_2 atmosphere. The medium was removed and the cells were washed once with PBS (1 mL). Cells were harvested with trypsin (1 mL, 0.1% *v/v*) for 5 minutes at 37 °C, and then media (1 mL) was added. Harvested cells were sedimented by centrifugation at 3000 rpm for 5 min, and then the supernatant removed. PBS (1 mL) was added to the cell pellet, which was then pipetted until a single cell suspension was achieved. The cells were re-sedimented by centrifugation. PBS (2 mL) was added to the cell pellet, which was then pipetted until a single cell suspension was achieved. An aliquot (100 μL) was taken for protein analysis. The remaining cells were sedimented by centrifugation at 3000 rpm for 5 min.

The mitochondria of the cell pellets were isolated using a reagent-based mitochondria isolation kit (Thermo Scientific Prod# 89874). At 4°C, the cell pellets were centrifuged at 12 000 rpm for 2 min and the supernatant removed. To the cell pellet 500 μL of reagent A was added, before mixing by means of vortex and incubation on ice for 2 minutes. Then 10 μL of reagent B was added before mixing by means of vortex and further incubation on ice with intermittent vortex mixing (every minute). 500 μL of Reagent C was added to the sample prior to centrifugation at 2900 rpm. The supernatant was transferred to a new vial, and the pellet was

retained for analysis. The supernatant was centrifuged at 12 000 rpm for 15 min. The supernatant was removed and retained as the cytosol fraction. The pellet was washed with a further 500 μL of reagent C, centrifuged at 12 000 rpm for 5 minutes and the supernatant discarded and the pellet retained as the mitochondrial fraction. These cell fractions were analysed for Gd content by means of ICP-MS.

Cell fractions were digested in HNO_3 (0.5 mL, 69%) at 65 °C in a water bath for 18 h. The digest was diluted to 10 mL with HCl (0.1 M), and then measured for Gd by means of ICP-MS. ICP-MS was run on a Perkin Elmer ELAN 6100 Inductively Coupled Plasma Emission Mass Spectrometer (ICP-MS) at the Solid State and Elemental Analysis Unit (UNSW Analytical Centre). Gd uptake concentrations are reported as ng Gd/mg protein.

Protein analyses

The bicinchoninic acid (BCA) protein assay was used to determine protein concentration, as described previously.[26] This assay relies on the reduction of alkaline Cu(II) by proteins. A bovine serum albumin (BSA) protein standard curve was prepared each time the assay was performed. Lysis of cells was achieved using three snap freeze–thaw cycles and cell debris was sedimented by centrifugation at 13 300 rcf for 5 min. The supernatant solution was then analysed for protein content by taking repeated 10 or 25 μL samples (N = 3 or 4) of the blank, 1 mg/mL BSA protein standard (200, 400, 800, and 1000 μg/mL, made up to volume with MQ water) or Gd-treated protein samples and depositing these into a 96-well plate format. Next, a freshly prepared solution of commercially sourced BCA and $CuSO_4 \cdot 5H_2O$ (50:1, 200 μL) was added to each well and the mixture was incubated at 37°C for 60 min. Absorbance was then measured at 600 nm using a Victor3V microplate reader (PerkinElmer) and protein was determined by comparison with the BSA standard curve.

Synchrotron X-ray fluorescence imaging

T98G human glioblastoma cells were grown directly on 500 nm thick Si_3N_4 windows (Silson Pty Ltd) and incubated for 24 h in the presence of 100 μM of **3**, **6** or **7** in MEM buffer (treated cells) or for 24 h with MEM buffer alone (control cells). Following incubation, the cells were washed with PBS buffer and the cells fixed to the window by dipping in MeOH at -78°C.

A549 human lung cancer cells were grown directly on 500 nm thick Si_3N_4 windows (Silson, Pty Ltd) and incubated for 24 h in the presence of 100 μM of **3** or **6** in MEM buffer (treated cells) or for 24 h with MEM buffer alone (control cells). Following incubation, the cells were fixed to the Si_3N_4 windows, by either one of two methods. In the first method, the silicon nitride windows were washed with PBS buffer and the cells fixed to the window by dipping in MeOH on dry ice. This method was used for sample windows of the control cells and cells treated with **3** and **6**. Additionally, a small number of sample windows containing cells treated with **6** were fixed using the second fixation method. In this method, the Si_3N_4 windows were washed with ammonium acetate solution (0.2 M), before flash freezing in a slurry of liquid N_2/*iso*-pentane. The windows were then freeze-dried overnight.

X-ray fluorescence imaging experiments were performed at the Australian Synchrotron. A monochromatic 10.2 keV X-ray[27] beam was focussed (to a spot size of 1 μm) using a zone plate, and the fluorescence signal was collected using a single-element silicon drift diode energy dispersive detector (Vortex EM, SII Nanotechnology), oriented at 73 degrees to the incident beam for 2 s per spatial point.

Individual cells were located using images obtained from an optical microscope positioned in the beamline downstream from the sample.[10, 28] Data were quantified (elemental area densities in μg/cm^2) using MAPS software[29] by fitting the full fluorescence spectrum at every spatial point to modified Gaussians[30] and comparing it with corresponding measurements on the thin-film standards NBS-1832 and NBS-1833 from the National Bureau of Standards (Gaithersburg, MD, USA).

[1]   a) J. Reedijk, *Curr. Opin. Chem. Biol.* **1999**, *3*, 236-240; b) P. Caravan, *Chem. Soc. Rev.* **2006**, *35*, 512-523; c) Z. Zhang, S. A. Nair and T. J. McMurry, *Curr. Med. Chem.* **2005**, *12*, 751-778.

[2]   A. H. Soloway, W. Tjarks, B. A. Barnum, F.-G. Rong, R. F. Barth, I. M. Codogni and J. G. Wilson, *Chem. Rev.* **1998**, *98*, 1515-1562.

[3]   a) S. Sjoberg, J. Carlsson, H. Ghaneolhosseini, L. Gedda, T. Hartman, J. Malmquist, C. Naeslund, P. Olsson and W. Tjarks, *J. Neurooncol.* **1997**, *33*, 41-52; b) S. C. Mehta and D. R. Lu, *Pharm. Res.* **1996**, *13*, 344-351; c) E. L. Crossley, E. J. Ziolkowski, J. A. Coderre and L. M. Rendina, *Mini-Rev. Med. Chem.* **2007**, *7*, 303-313.

[4]   B. H. Laster, W. C. Thomlinson and R. G. Fairchild, *Radiat. Res.* **1993**, *133*, 219-224.

[5]   a) W. Chen, S. C. Mehta and D. R. Lu, *Adv. Drug Delivery Rev.* **1997**, *26*, 231-247; b) D. P. Gierga, J. C. Yanch and R. E. Shefer, *Med. Phys.* **2000**, *27*, 1685-1692; c) J. Stepanek, *Med. Phys.* **2003**, *30*, 41-43; d) G. De Stasio, D. Rajesh, P. Casalbore, M. J. Daniels, R. J. Erhardt, B. H. Frazer, L. M. Wiese, K. L. Richter, B. R. Sonderegger, B. Gilbert, S. Schaub, R. J. Cannara, J. F. Crawford, M. K. Gilles, T. Tyliszczak, J. F. Fowler, L. M. Larocca, S. P. Howard, D. Mercanti, M. P. Mehta and R. Pallini, *Neurol. Res.* **2005**, *27*, 387-398; e) R. C. Greenwood, C. W. Reich, H. A. Baader, H. R. Koch, D. Breitig, O. W. B. Schult, B. Fogelberg, A. Backlin, W. Mampe and et al., *Nucl. Phys. A* **1978**, *A304*, 327-428.

[6]   a) J.-F. Adam, A. Joubert, M.-C. Biston, A.-M. Charvet, M. Peoc'h, J.-F. Le Bas, J. Balosso, F. Esteve and H. Elleaume, *Int. J. Radiat. Oncol.* **2006**, *64*, 603-611; b) M.-C. Biston, A. Joubert, J.-F. Adam, H. Elleaume, S. Bohic, A.-M. Charvet, F. Esteve, N. Foray and J. Balosso, *Cancer Res.* **2004**, *64*, 2317-2323; c) J. F. Adam, M. C. Biston, J. Rousseau, C. Boudou, A. M. Charvet, J. Balosso, F. Esteve and H. Elleaume, *Phys. Med.* **2008**, *24*, 92-97.

[7]   G. De Stasio, D. Rajesh, J. M. Ford, M. J. Daniels, R. J. Erhardt, B. H. Frazer, T. Tyliszczak, M. K. Gilles, R. L. Conhaim, S. P. Howard, J. F. Fowler, F. Esteve and M. P. Mehta, *Clin. Cancer Res.* **2006**, *12*, 206-213.

[8] a) R. F. Martin, G. D'Cunha, M. Pardee and B. J. Allen, *Int. J. Radiat. Biol.* **1988**, *54*, 205-208; b) R. F. Martin, G. D'Cunha, M. Pardee and B. J. Allen, *Pigm. Cell Res.* **1989**, *2*, 330-332.

[9] a) T. Goorley and H. Nikjoo, *Radiat. Res.* **2000**, *154*, 556-563; b) T. Goorley, R. Zamenhof and H. Nikjoo, *Int. J. Radiat. Biol.* **2004**, *80*, 933-940.

[10] E. L. Crossley, J. B. Aitken, S. Vogt, H. H. Harris and L. M. Rendina, *Angew. Chem. Int. Ed.* **2010**, *49*, 1231-1233.

[11] a) J. M. Ford, W. Seiferheld, J. R. Alger, G. Wu, T. J. Endicott, M. Mehta, W. Curran and S.-C. Phan, *Int. J. Radiat. Oncol.* **2007**, *69*, 831-838; b) P. Carde, R. Timmerman, M. P. Mehta, C. D. Koprowski, J. Ford, R. B. Tishler, D. Miles, R. A. Miller and M. F. Renschler, *J. Clin. Oncol.* **2001**, *19*, 2074-2083; c) D. I. Rosenthal, P. Nurenberg, C. R. Becerra, E. P. Frenkel, D. P. Carbone, B. L. Lum, R. Miller, J. Engel, S. Young, D. Miles and M. F. Renschler, *Clin. Cancer Res.* **1999**, *5*, 739-745; d) M. P. Mehta, W. R. Shapiro, S. C. Phan, R. Gervais, C. Carrie, P. Chabot, R. A. Patchell, M. J. Glantz, L. Recht, C. Langer, R. K. Sur, W. H. Roa, M. A. Mahe, A. Fortin, C. Nieder, C. A. Meyers, J. A. Smith, R. A. Miller and M. F. Renschler, *Int. J. Radiat. Oncol.* **2009**, *73*, 1069-1076; e) K. A. Bradley, I. F. Pollack, J. M. Reid, P. C. Adamson, M. M. Ames, G. Vezina, S. Blaney, P. Ivy, T. Zhou, M. Krailo, G. Reaman and M. P. Mehta, *Neuro-oncol.* **2008**, *10*, 752-758.

[12] D. E. Morrison, J. B. Aitken, M. D. de Jonge, J. A. Ioppolo, H. H. Harris and L. M. Rendina, *Chem. Commun.* **2014**, *50*, 2252-2254.

[13] a) J. S. Modica-Napolitano and J. R. Aprille, *Adv. Drug Delivery Rev.* **2001**, *49*, 63-70; b) J. A. Ioppolo, J. K. Clegg and L. M. Rendina, *Dalton Trans.* **2007**, 1982-1985; c) J. A. Ioppolo, M. Kassiou and L. M. Rendina, *Tetrahedron Lett.* **2009**, *50*, 6457-6461; d) D. E. Morrison, F. Issa, M. Bhadbhade, L. Groebler, P. K. Witting, M. Kassiou, P. J. Rutledge and L. M. Rendina, *J. Biol. Inorg. Chem.* **2010**, *15*, 1305-1318; e) Y.-S. Kim, C.-T. Yang, J. Wang, L. Wang, Z.-B. Li, X. Chen and S. Liu, *J. Med. Chem.* **2008**, *51*, 2971-2984; f) J. Wang, C.-T. Yang, Y.-S. Kim, S. G. Sreerama, Q. Cao, Z.-B. Li, Z. He, X. Chen and S. Liu, *J. Med. Chem.* **2007**, *50*, 5057-5069; g) Y. Zhou and S. Liu, *Bioconjug. Chem.* **2011**, *22*, 1459-1472.

[14] a) J. D. Steichen, M. J. Weiss, D. R. Elmaleh and R. L. Martuza, *J. Neurosurg.* **1991**, *74*, 116-122; b) I. Madar, J. H. Anderson, Z. Szabo, U.

[15] Scheffel, P.-F. Kao, H. T. Ravert and R. F. Dannals, *J. Nucl. Med.* **1999**, *40*, 1180-1185.

[15] J. S. Modica-Napolitano and J. R. Aprille, *Cancer Res.* **1987**, *47*, 4361-4365.

[16] V. M. Runge, D. M. Kaufman, M. L. Wood, L. S. Adelman and S. Jacobson, *Int. J. Rad. Appl. Instrum. B* **1989**, *16*, 561-567.

[17] a) E. Brucher, *Top. Curr. Chem.* **2002**, *221*, 103-122; b) A. E. Martell, R. J. Motekaitis, E. T. Clarke, R. Delgado, Y. Sun and R. Ma, *Supramol. Chem.* **1996**, *6*, 353-363.

[18] C. Chen and B. H. Paw, *Biochim. Biophys. Acta, Mol. Cell Res.* **2012**, *1823*, 1459-1467.

[19] D. F. Schriver, *The Manipulation of Air-Sensitive Compounds*, McGraw-Hill, New York, **1969**.

[20] W. L. F. Armarego and C. Chai, *Purification of Laboratory Chemicals, 5th Edition*, **2003**.

[21] P. S. Athey and G. E. Kiefer, *J. Org. Chem.* **2002**, *67*, 4081-4085.

[22] D. A. Moore, *Org. Synth.* **2008**, *85*, 10-14.

[23] P. Caravan, C. T. Farrar, D. Frullano and U. Ritika, *Contrast Media Mol. Imaging* **2009**, *4*, 80-100.

[24] H. B. Eldredge, M. Spiller, J. M. Chasse, M. T. Greenwod and P. Caravan, *Invest. Radiol.* **2006**, *41*, 229-243.

[25] T. Mosmann, *J. Immunol. Methods* **1983**, *65*, 55-63.

[26] P. K. Smith, R. I. Krohn, G. T. Hermanson, A. K. Mallia, F. H. Gartner, M. D. Provenzano, E. K. Fujimoto, N. M. Goeke, B. J. Olson and D. C. Klenk, *Anal. Biochem.* **1985**, *150*, 76-85.

[27] D. Paterson, M. D. de Jonge, D. L. Howard, W. Lewis, J. McKinlay, A. Starritt, M. Kusel, C. G. Ryan, R. Kirkham, G. Moorhead and D. P. Siddons, *AIP Conf. Proc.* **2011**, *1365*, 219−222.

[28] a) E. A. Carter, B. S. Rayner, A. I. McLeod, L. E. Wu, C. P. Marshall, A. Levina, J. B. Aitken, P. K. Witting, B. Lai, Z. Cai, S. Vogt, Y.-C. Lee, C.-I. Chen, M. J. Tobin, H. H. Harris and P. A. Lay, *Mol. Biosyst.* **2010**, *6*, 1316-1322; b) C. M. Weekley, J. B. Aitken, S. Vogt, L. A. Finney, D. J. Paterson, M. D. de Jonge, D. L. Howard, P. K. Witting, I. F. Musgrave and H. H. Harris, *J. Am. Chem. Soc.* **2011**, *133*, 18272-18279.

[29] S. Vogt, *J. Phys. IV,* **2003**, *104*, 635-638.

[30] P. van Espen in *Handbook of X-ray spectrometry: Revised and expanded,* (Eds.: R. van Grieken and A. Markowicz), Dekker, New York, **2002**.

Entry for the Table of Contents

FULL PAPER

A library of new, bifunctional Gd(III) complexes has been evaluated to address many key criteria for cutting-edge binary therapies such as photon activation therapy and neutron capture therapy. The highest *in vitro* tumor selectivity for any Gd agent is also reported.
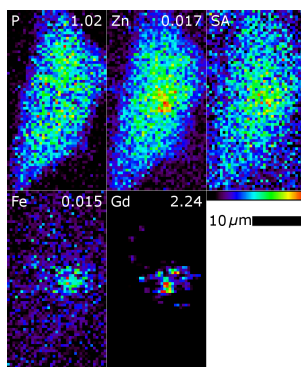
Daniel E. Morrison, Jade B. Aitken, Martin D. de Jonge, Fatiah Issa, Hugh H. Harris and Louis M. Rendina*

Page No. – Page No.

Synthesis and biological evaluation of a new class of mitochondria-targeted gadolinium(III) agents